Chapter 1

RECENT RESULTS FROM THE CERES/NA45 EXPERIMENT AND UPGRADE WITH A RADIAL-DRIFT TPC

ShinIchi Esumi for the CERES/NA45 collaboration
Physikalisches Institut, Universität Heidelberg
Philosophenweg 12, D-69120 Heidelberg, Germany
esumi@ceres1.physi.uni-heidelberg.de

Abstract The CERES/NA45 experiment measures low mass electron pair production in Pb-Au collisions at 158AGeV at the CERN SPS. In this paper, we present the electron pair enhancement in the mass range $0.2 < m_{ee} < 0.7$ GeV/c^2, it increases more than linear with charged multiplicity and is most pronounced at low pair $p_T < 0.5$ GeV/c. Transverse mass and rapidity distributions for charged hadrons $h^+ - h^-$ and azimuthal event anisotropies (v_1, v_2) of charged particles are shown as a function of centrality. Finally, we present the status of the upgrade with a radial-drift TPC.

Keywords: QGP, CERES, RICH, TPC, dilepton

1. INTRODUCTION

CERES is an experiment dedicated to the measurement of low-mass electron pair production in heavy-ion collisions at SPS energy. The production of dileptons is expected to convey information from the early stage of the collisions where quark-gluon-plasma (QGP) formation and restoration of chiral symmetry might happen. The CERES spectrometer is optimized to measure electron pairs from 50 MeV/c^2 up to 2 GeV/c^2 at mid-rapidity $2.1 < \eta < 2.65$ with 2π azimuthal coverage. The collision point (vertex) is determined by two silicon drift chambers (SDC) located just behind the target. Two ring imaging Cherenkov detectors (RICH) with methane gas radiator ($\gamma_{th} \sim 32$, which makes it blind to most of the hadrons) are used to identify electrons. A pad chamber (PC) behind the two RICH detectors, in conjunction with all other detectors, is used to track the particles. In between the two RICH detectors, there is a superconducting double solenoidal magnet to provide an azimuthal deflection for momentum / charge measurement of the tracks.

2. ELECTRON PAIR PRODUCTION

CERES has measured electron pair production in p-A collisions at the SPS and found that it is well explained by the decay of hadrons whose abundancies have been measured [1]. On the other hand, in sulphur and lead induced heavy-ion collisions, production of electron pairs has been found to be enhanced relative to the expected contributions from hadrons decays [2, 3].

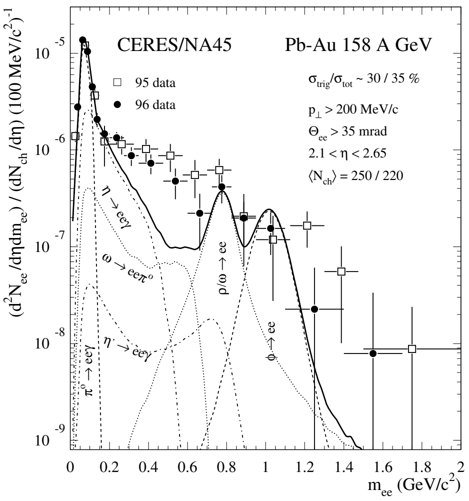

Figure 1.1 Electron pair mass spectra normalized to charged particle multiplicity. Two different symbols represent the data sets from the different years for the same system 158AGeV Pb-Au. The expected electron pair yield from hadron decays at freeze out is shown as the solid line, the different source contributions are shown as the dashed lines.

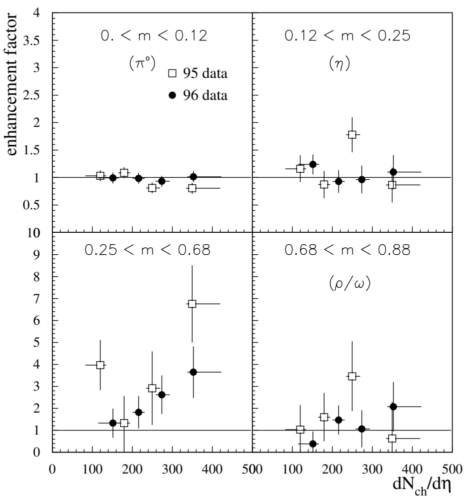

Figure 1.2 Centrality dependence of the enhancement factor relative to the expected yield ($N^{e^+e^-}_{measured}$ / $N^{e^+e^-}_{hadronic\ sources}$) for 4 different mass windows. Linear increase (quadratic increase with charged multiplicity, since $N^{e^+e^-}_{hadronic\ sources}$ is proportional to the charged multiplicity) is observed only within the mass window $0.25 < m_{ee} < 0.68$ GeV/c^2.

After background rejection cuts, an inclusive e^+e^- mass spectrum for 158AGeV Pb-Au collisions is obtained by subtracting the geometric mean of the like sign pair spectrum from the unlike sign pair spectrum. The result is shown in Fig. 1.1 for the data sets from the 1995 and

1996 runs. The invariant mass spectrum is in good agreement with the expectations for hadron decays below 200 MeV/c^2 where the expected sources are dominanated by π^0 and η Dalitz decays. For masses above 200 MeV/c^2, an enhancement of electron pair production is clearly seen in the mass region up to the ρ, ω peak compared to the expected contribution from hadronic sources as shown in Fig. 1.1. The enhancement factor, integrating over the mass range $0.25 < m_{ee} < 0.7$ GeV/c^2, is $2.6 \pm 0.5(stat.) \pm 0.5(syst.)$ for the '96 data and $3.9 \pm 0.9(stat.) \pm 0.9(syst.)$ for the '95 data [4, 5].

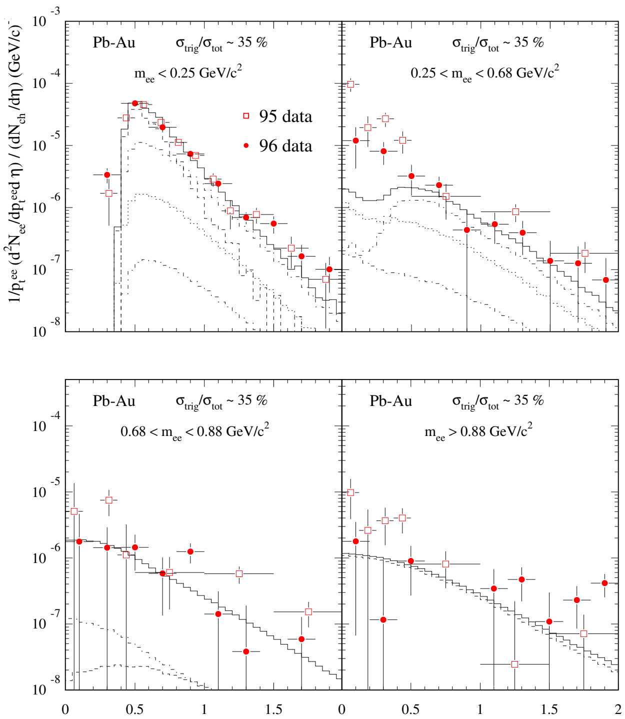

Figure 1.3 Inclusive e$^+$e$^-$ pair p_T spectra in GeV/c for 4 different mass windows, which show the observed enhancement is within the mass window $0.25 < m_{ee} < 0.68$ GeV/c^2 and mostly from the low pair p_T region $<$ 0.5 GeV/c.

The effect has been studied as a function of centrality as shown in Fig. 1.2. If hadron decays are the only source of dielectron pairs, as is the case in p-p and p-A collisions, the data should scale linearly with charged multiplicity, as indicated by the horizontal line in Fig. 1.2. The data clearly indicate a stronger than linear dependence as a function of charged multiplicity within the mass window $0.25 < m_{ee} < 0.68$ GeV/c^2. Inclusive e$^+$e$^-$ pair p_T spectra are shown in Fig. 1.3 for 4 different mass windows. Our single particle p_T cut ($p_T > 200$ MeV/c) strongly affects the pair p_T distribution for masses below 400 MeV/c^2 at low pair p_T. The hadronic decay generator curves shown are folded with such kinematical cuts and the momentum resolution. The measured enhancement within the mass window $0.25 < m_{ee} < 0.68$ GeV/c^2 is most pronounced in the low pair p_T region at $p_T < 0.5$ GeV/c.

3. CHARGED HADRON DISTRIBUTIONS

The two silicon drift chambers just behind target and before the magnetic field and pad chamber after the magnetic field are used to allow charged particle tracking. By subtracting the negatively charged particle

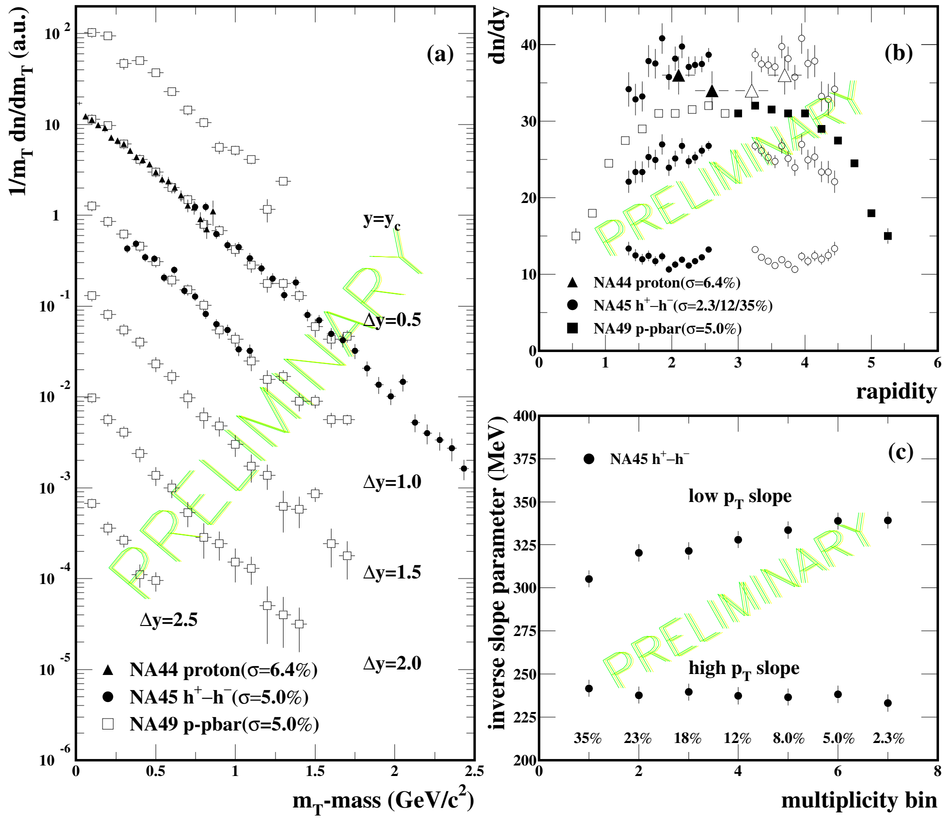

Figure 1.4 Part(a) shows the $(h^+ - h^-)$ transverse mass distribution at 158AGeV Pb-Au collisions (circle) compared with identified proton transverse mass distributions in 158AGeV Pb-Pb collisions from NA44 (triangles)[8] and $(p - pbar)$ transverse mass distribution from NA49 (squares)[9]. Part(b) shows the rapidity distribution of $(h^+ - h^-)$ for different centralities compared to similar results from two other experiments. Part(c) shows the fitted inverse slope parameters as a function of the centrality of the collision. The fitting is done with two exponential functions. The upper(lower) data points represent the lower(higher) $m_T - m_p$ region < 0.7GeV/c($>$ 0.7GeV/c).

distribution from the positively charged particle distribution and using the proton mass, transverse mass and rapidity distribution of $(h^+ - h^-)$ (related to the net proton distributions) are studied as a function of the centrality in 158AGeV Pb-Au collisions shown in Fig. 1.4. The first results were shown in [6, 7]. Within the angular (θ) acceptance of the CERES spectrometer which corresponds for protons to the rapidity acceptance $1.0 < y_p < 2.6$ with a varying transverse momentum coverage $m_T - m_p < 2$ GeV/c^2, the shape of the transverse mass and rapidity distributions of $(h^+ - h^-)$ are investigated here with the main emphasis to study the stopping power in 158AGeV Pb-Au collisions. The change of rapidity distribution from mid-central to central collisions in terms of yield and shape shows an increase of stopping power as a function of centrality as seen in Fig. 1.4(b). The data shows a better fit with two exponential functions than with single exponential function. The shape of transverse mass distribution at lower p_T region $m_T - m_p < 0.7$ GeV/c^2 is flattening with increasing centrality, while the inverse slope parameter in the higher p_T region $m_T - m_p > 0.7$ GeV/c^2 is unchanged with increasing centrality seen in Fig. 1.4(c).

Following the method outlined in [10, 11, 12, 13] a Fourier analysis of the azimuthal charged particle distribution is done with respect to the reaction plane. The directed (v_1) and elliptic (v_2) flow coefficients are measured as a function of pseudorapidity and as a function of centrality as shown in Fig. 1.5. We have chosen a negative sign of v_1 in the forward hemisphere, since the dominant charged particles are pions which are measured to be negative with respect to the proton flow in the other experiments at the same energy [14, 15]. Both v_1 and v_2 are decreasing from $3-5\%$ at mid-central (30%) down to about 1% at central collisions (5%).

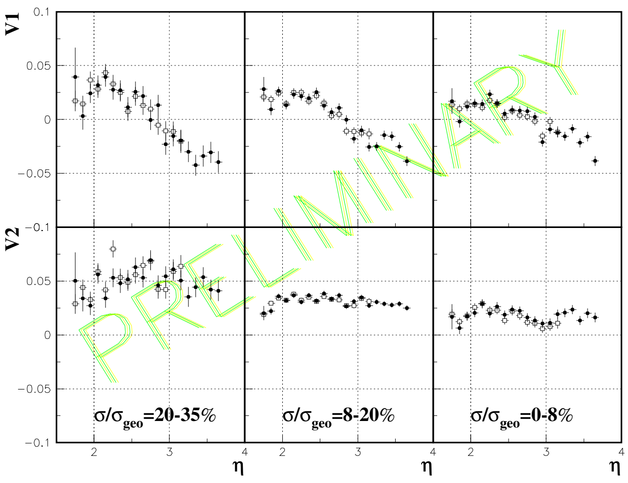

Figure 1.5 Flow parameters v_1 and v_2 as a function of pseudorapidity for different centrality. The reaction plane is determined by two independent subsamples of hits in SDC1. The solid symbols are coefficients calculated for hits in SDC1 and the open symbols are for SDC2. Autocorrelations are avoided by using the reaction plane from another sub-sample. Correction for the reaction plane resolution are applied.

4. UPGRADE WITH RADIAL-DRIFT TPC

The CERES spectrometer has been upgraded by the addition of radial-drift time projection chamber (TPC) with an additional magnetic field behind the RICH detectors. The new experimental setup is shown in Fig. 1.6. The TPC has a cylindrical geometry as all the other detectors in the experiment and covers the same angular acceptance in θ. Electrons produced by inonization due to the passage of charged particles in the TPC are drifted in a radial electric field defined by an inner cylindrical electrode and 16 read-out chambers at out side. The read-out chambers are multiwire proportional chambers with cathode pad read-out. There are 20 pad-rows in beam (z) direction with 16×48 pads in azimuthal direction, each sampling the radial (drift) direction in 256 time bins. A magnetic field is provided by two large coils surrounding the TPC with currents running in opposite direction. The measurement of track curving through the magnetic field will provide momentum of the track. The TPC in conjunction with the two SDC's will significantly improve the dielectron mass resolution less than 2% at the ω mass.

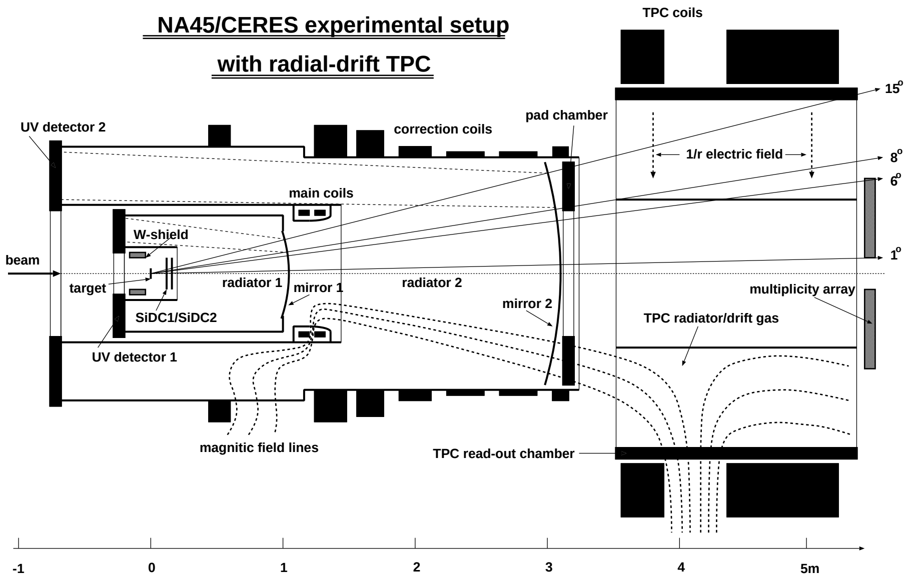

Figure 1.6 CERES/NA45 Experimental setup for '98 and '99 run with radial-drift TPC behind the RICH spectrometer

The goal is to achieve a momentum resolution which allows the experiment to be sensitive to the width of ω and ϕ mesons. The dielectron mass spectrum expected from hadronic decays is shown in Fig. 1.7. Here unchanged natural widths are used for the ρ, ω, ϕ mesons. The TPC was

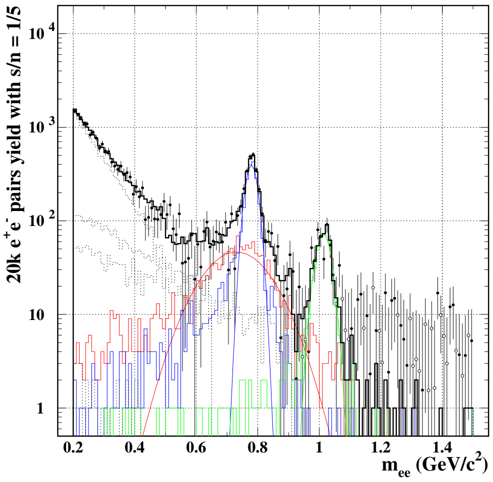

Figure 1.7 Expected electron pair mass spectrum from upgraded CERES/NA45 spectrometer with the radial-drift TPC is calculated by assuming a statistics of 20k pairs with signal to noise ratio at 1/5 in the masses above 200 MeV/c^2.

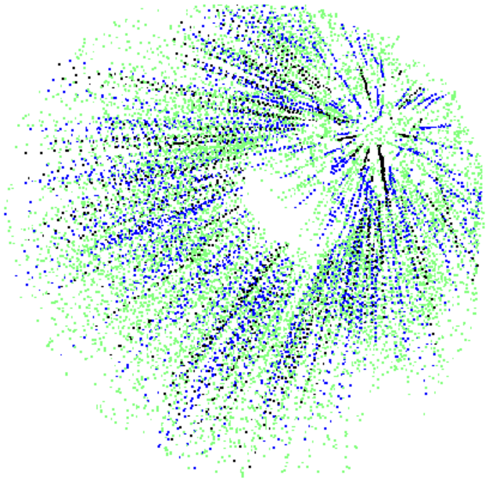

Figure 1.8 158AGeV central Pb-Au event display of the TPC looking from the downstream end of the TPC; all hits are displayed and track segments in the TPC are clearly recognizable.

operational in an engineering run in November 1998 and a typical event display from one central Pb-Au collision is shown in Fig. 1.8.

5. SUMMARY

Electron pair production in 158AGeV Pb-Au collisions is enhanced about quadratically in the mass region $0.2 < m_{ee} < 0.7$ GeV/c^2 and most pronounced in the low pair p_T region < 0.5 GeV/c. CERES has also measured hadronic variables: charged hadron distributions and azimuthal event anisotropies. Our plan is to study the correlation between those different variables including measured leptons. A Radial-drift TPC has been build in order to improve the mass resolution and first test runs with laser/muon/p-Pb/Pb-Au triggers have been performed during 1998. Analysis of those runs is now in progress and a low energy heavy ion run at 40AGeV Pb-Au is planned for 1999 to investigate dilepton production at higher baryon and lower energy density.

Acknowledgments

The authors wish to thank for the good performance of the CERN PS and SPS accelerators. We are grateful for financial support by the German BMBF, the U.S. DoE, the MINERVA Foundation, the German-Israeli Foundation for Scientific Research and Development, and the Israeli Science Foundation.

References

[1] G.Agakichiev et al., CERES collaboration, Eur. Phys. J. **C4**, (1998) 431.

[2] G.Agakichiev et al., CERES collaboration, Phys. Rev. Lett. **75**, (1995) 1727.

[3] G.Agakichiev et al., CERES collaboration, Phys. Lett. **B422**, (1998) 405.

[4] B.Lenkeit, Doctoral Thesis, Heidelberg (1998).

[5] B.Lenkeit et al., CERES collaboration, Proc. International Nuclear Physics Conference, Paris, August 1998, Nucl. Phys. **A** in print.

[6] F.Ceretto, Doctoral Thesis, Heidelberg (1998).

[7] F.Ceretto et al., CERES collaboration, Nucl. Phys. **A638**, (1998) 467c.

[8] I.G. Bearden et al., NA44 Collaboration, Phys. Lett. **B388**, (1996) 431.

[9] P.G.Jones et al., NA49 Collaboration, Nucl. Phys. **A610**, (1996) 188c.

[10] J.Barrette et al., E877 Collaboration, Phys. Rev.Lett. **73**, (1994) 2532.

[11] J.Barrette et al., E877 Collaboration, Phys. Rev. **C55**, (1997) 1420.

[12] J.Barrette et al., E877 Collaboration, Phys. Rev. **C56**, (1997) 3254.

[13] A.Poskanzer and S.Voloshin, Phys. Rev. **C58**, (1998) 1671.

[14] S.Nishimura et al., WA98 Collaboration, Nucl. Phys. **A638**, (1998) 459c.

[15] A.Poskanzer et al., NA49 Collaboration, Nucl. Phys. **A638**, (1998) 463c.